1-10-2023

Using Dielectric Scatters to Selectively Excite Embedded Eigenstates in Cavity Resonators

Olugbenga Joshua Gbidi
Rowan University

USING DIELECTRIC SCATTERS TO SELECTIVELY EXCITE EMBEDDED EIGENSTATES IN CAVITY RESONATORS

by

Olugbenga J. Gbidi

A Thesis

Submitted to the
Department of Mechanical Engineering
Henry M. Rowan College of Engineering
In partial fulfillment of the requirement
For the degree of
Master of Science in Mechanical Engineering
at
Rowan University
December 16, 2022

Thesis Advisor: Chen Shen, Ph.D., Assistant Professor, Department of Mechanical Engineering

Committee Members:
Ratneshwar Jha, Ph.D., Professor, Head of Department of Mechanical Engineering

Ben Wu, Ph.D., Assistant Professor, Department of Electrical & Computer Engineering

Dedication

I would like to dedicate this thesis to my late grandparents who taught me to always do my best and go the extra distance. My friends who supported me in any decision I made with assistance and encouragement along the way. My family who knew I would succeed in anything I try and were always there to listen. Especially to my mother, Titilayo Gbidi, who taught me that progress begins with you taking a step, no matter how large, and with dedication there is nothing you cannot do. I would not be here without those around me. Thank you.

Acknowledgements

I would like to acknowledge my committee chair and advisor, Dr. Chen Shen, for his help and guidance throughout this journey. Dr. Shen's patience and determination was exactly the support the project needed.

Abstract

Olugbenga J. Gbidi
USING DIELECTRIC SCATTERS TO SELECTIVELY EXCITE EMBEDDED EIGENSTATES IN CAVITY RESONATORS
2021-2022
Chen Shen, Ph.D.
Master of Science in Mechanical Engineering

Bound states in the continuum (BICs) are waves that remain in the continuous spectrum of radiating waves that carry energy, however, still localized within the spectrum. BICs, also embedded eigenmodes, exhibit high quality factors that have been observed in optical and acoustic waveguides, photonic structures, and other material systems. Presently, there are limited means to select these BICs in terms of the quality factor and their excitation. In this work, we show that a different type of BIC, Quasi-BICs (Q-BICs), in open resonators can have their quality attuned by introducing embedded scatters. Using microwave cavities and dielectric scatters as an example, we show that by tuning the geometry of the structure and the specific locations of the dielectric scatters Q-BICs can be selectively chosen to exhibit enhancements to their quality. The coupled mode theory (CMT) and numerical simulations are employed to inspect the altering of dielectrics, structure parameters, and tuning of the quality factor for the Q-BICs chosen. These results may be beneficial to the application of enhanced optical lasers, sensors, open structures that need contained radiation and control over selectivity.

Table of Contents

Table of Contents (Continued)

List of Figures

Chapter 1

Introduction

In modern science and technology, the ability to confine light and realize optical states with large oscillation lifetime is of high importance. The partial or complete containment of waves is present in nature and in wave-based technology. Demonstrations include a variety of scenarios, such as for filtering, sensing, enhancement of light–matter interactions, light contained in long-range optical communications, and the partial confinement of sound in musical instruments. The allowed frequencies of oscillation are known as the wave spectrum.

Bound states in the continuum (BICs) were first proposed in the 1920s. BICs are known to be embedded eigenstates or eigenmodes at a specific frequency. Ideal BICs lie within the spectrum and energy does not radiate which means it maintains an infinitely large quality factor. Theoretically, the quality factor approaches infinity for BICs since the energy is fully trapped. This is what is generally known from studies and previous experiments considering this wave phenomena.

This thesis studies the interaction between quasi-BICs in electromagnetic (EM) waves and embedded dielectric scatters in microwave cavity resonators. Previous works has shown the existence of bound states and characteristics of various geometry structures that can support them. However, the work here develops a general groundwork for ability to selectively excite specific quasi-BICs.

1.1 Motivation

Quasi-bound states are known to be the one of the closest representations of bound states in experimental scenarios. Bound states have been studied in other systems; however, it is only recently that characteristics and effects are being observed for similarities. The overall exchange of effects between the magnetic field and dielectric materials is not heavily examined in cavity resonators. Previously bound states were limited to be seen in systems such as water waves and acoustic waves.

As technology grows, so does the need for understanding these bound states in other systems to be utilized for practical purposes. In addition, the variability between these systems brings the need to understand if effects can be replicated and tuned critically.

The motivation for the work presented in this thesis is to expand on an understanding of Q-BICs and the interaction that dielectric materials can give rise to. Many papers and studies focus on enhancing specific types of BICs. Others have concentrated on finding higher Q-factors in bound states in specific resonator shapes. Studies have aimed to minimize cavity sizes for tailoring specifics cases. There are not many studies focused on bound states that have explored the ability to choose certain modes to strengthen or suppress. The importance of this study is that these Q-BICs support high quality for photonic crystal structures, fiber communications, and many other fields.

1.2 Objectives

The aims of this research work presented in this thesis are:

1. Identify characteristics and key parameters in cavity resonators and design a structure that support embedded eigenmodes;

2. Expand upon the structure to study interaction to dimensions along with embedded materials;
3. Utilize numerical simulations and established theories in comparisons to verify symmetry parameters.

A combination of numerical simulations with the support of the finite element method and computational processing to accomplish accurate comparisons. It is anticipated that replicating these structures can demonstrate reinforcement for Q-BICs.

1.3 Scope and Organization of the Thesis

This thesis is organized as follows. Chapter 1 introduces BICs and their importance. Chapter 2 will present a comprehensive literature review of the existence of BICs in other works and various techniques that are implemented in this thesis. Chapter 3 discusses the design and shape of the structure, choice of materials, and how I will be verifying each Q-BIC configuration with the coupled-mode theory and numerical simulations. Chapter 4 presents the results found from COMSOL and compared with MATLAB for analysis. Chapter 5 discusses conclusions from results and contributions from this thesis, future work recommendations.

Chapter 2

Background

There is much on the existence in optical fields, symmetry characteristics, acoustic, and interactions with metamaterials, however literature is lacking for the selectivity of modes. This section will serve as a literary survey of wave phenomena prior to existing bound states found in other works for various structures. Background on the foundation and their applications in different fields is covered as well. Techniques used to verify results and findings are discussed for their parameters and characteristics.

A similar phenomenon, a predecessor, that was studied and observed prior to bound states are trapped modes. These trapped modes are known to be eigenfunctions whose eigenvalues are embedded in the continuous spectrum, for certain obstacles which are symmetrical with respect to reflections in the centerline of a two-dimensional waveguide [1]. Such a mode is a free oscillation of an unbounded fluid with a free surface that has finite energy, does not radiate waves to infinity, and in the absence of viscosity will persist for all time [2]. An extension of trapped modes goes into water waves, within the linearized theory of water waves, certain structures when held fixed can support a trapped mode of a particular frequency [2]. A freely floating structure and a trapped mode is a coupled oscillation of the surrounding fluid and the structure. It is possible to design a fully numerical scheme to search for complex resonances for waveguide problems and this has been done by applying perfectly matched layer (PML) absorbing boundary conditions, which reduce the problem to one on a finite 4 and separate the discrete resonances from the continuous spectrum [3]. Mathematically, they can be thought of as eigenvectors corresponding to eigenvalues of certain differential

operators on unbounded domains. Eigenvalues are special cases of complex resonances in which the imaginary part is zero. The existence of eigenvalues that are embedded in the continuous spectrum is much more difficult to establish and they are much harder to locate. From the practical point of view, the existence of a trapped mode means that it is crucial to find accurate numerical solutions to the radiation and scattering problems for a range of frequencies around the trapped mode frequency. Embedded eigenmodes for several simple geometries have been established, but the only general procedure that is available is to compute the complex resonances for the problem numerically and then look for parameter values at which one or more of these resonances have zero imaginary part. Doing this is possible, however very limited in choices of resonances. Recently there has been studies into free-floating structures and their interplay with trapped modes. Past works have demonstrated that although trapped modes supported by a fixed structure, cannot be excited when that structure is allowed to float freely. However, McIver and Fitzgerald, show that certain structures that support such modes are termed, motion trapping structures, and can be contrasted with the previously-known sloshing trapping structures that, when held fixed, can support free oscillations of the fluid [2]. Further examination shows that equations of motion shows that motion-trapped modes cannot be excited by incident waves, but they can be excited by giving the structure a non-zero initial displacement. Evidence of trapped modes can be found in water waves and acoustics, both being expanded to more interesting wave phenomena [1–6].

Bound states in the continuum (BICs) were first proposed and mathematically proved by John von Neumann and Eugene Wigner in the 1920s [7]. Bound states are a wave phenomenon is observed first in quantum mechanics, there is demonstrations in

different systems such as photonic crystal systems [1,3,12–18,4–11], acoustic waves [18–22], water waves [22–26], and in recent years electromagnetic waves [2,6,31,32,8,14,18,25,27–30]. BICs are known to be embedded eigenstates, eigenmodes, or waves propagating in the system where energy lies in the spectral range, but at a specific frequency. The difference between ideal BICs and leaky resonances is that it lies within the spectrum and energy does not radiate which means it maintains an infinitely large quality factor. The quality factor evaluates the resonance quality in proportional relation of energy stored to energy dissipated. Theoretically, the quality factor approaches infinity for ideal BICs since the energy is fully trapped [9]. For wave systems, an indicator of the BICs could be the complex eigenfrequency which is defined as the eigenvalue of the wave equation with the outward boundary conditions [9]. The imaginary part of the complex eigenfrequency indicates the radiative decay rate [9]. BICs that remain in the continuum have exceptionally low decay rates, the imaginary part then vanishes, and higher Q-factors are exhibited. Inside the continuum, resonances may be found that locally resemble a bound state but in fact couple to the extended waves and leak out; they can be associated with a complex frequency, $\omega = \omega_0 - i\gamma$, in which the real part ω_0 is the resonance frequency and the imaginary part γ represents the leakage rate. This complex frequency is defined rigorously as the eigenvalue of the wave equation. In a scattering experiment, waves coming in from infinity can excite the resonances, causing a rapid variation in the phase and amplitude of the scattered waves. However, such waves cannot excite BICs, because BICs are completely decoupled from the radiating waves coming from infinity. Theoretically proposed and observed BICs are in extended structures because, in most wave systems, BICs are forbidden in compact structures.

Structures that support BICs are extended, many are uniform or periodic in one or more directions (i.e., x and y) and the BIC localizes in the other direction (i.e., z). The unique properties of BICs have led to numerous applications, including lasers, sensors, filters and low-loss fibers, with many more possible uses proposed and yet to be implemented [9].

2.1 Types of BICs and Properties

There is more than one type of BICs, some being higher order compared to others [1,2,15–24,3,25–33,8–14]. Different types of BICs include symmetry-protected BICs, the Friedrich-Wintgen BIC and quasi-BICs. The type of BIC a structure can support depends on many parameters such as the geometry, the material, and the resonance frequency as well. The ways that these BICs are induced each vary as varying certain parameters will affect one BIC and not the other similarly [9,10,21–25,32–36,11–13,16–20].

2.1.1 Symmetry-Protected BIC

Symmetry-protected BICs (SP BICs) arise just like the name implies, when a system exhibits a reflection or rotational symmetry, modes of different symmetry classes completely decouple. A common setup is a 1D waveguide that supports a continuum of even extended states, with two defects attached symmetrically above and below this array to create an odd defect bound state. When the mirroring symmetry is broken the BIC turns into a leaky resonance, from this there are ways to break the symmetry and tune the radiation [9]. A temperature gradient can change the refractive index of the material and

break the mirror symmetry, which alter radiation in a controllable way. Recent works have shown experimentally that a mirror symmetry is not a necessary condition for a BIC formation. Van Hoof et al. show that it is possible to excite SP BICs and directly image the spatial distribution of their associated EM fields. Only π-rotation symmetry is required, making BICs exceptionally robust to structural changes and makes SP BICs exceptionally robust to relative displacements of the scatterers, which makes the fabrication of open resonant cavities with high Q-factors simple [31]. By displacing the scatterers in the dimer, the mirror symmetry of the metasurface is broken and they show experimentally that only π-rotation symmetry is necessary to sustain SP BICs. The arrangement of these structures in a photonic lattice can tailor their radiation properties to enhance the scattering in certain directions which is related to lasing applications I will discuss in following sections.

2.1.2 Friedrich-Wintgen BIC

Friedrich-Wintgen BIC (FW) is a type of BIC that was found by Friedrich and Wintgen as a general way to find BICs in a quantum system. When two resonance states approach each other as a function of a continuous parameter, interference causes an avoided crossing of the two states in their energy positions and, for a certain value of the parameter, the narrow linewidth of one of the resonance states may vanish exactly. Since it remains above the threshold for decay into the continuum, this state becomes a BIC although each resonant state has a finite width [20]. The first examples of Friedrich–Wintgen BICs were proposed in atoms and molecules, but further studies extend to acoustics, they have been studied in multi-resonant cavities. In optics, they have been

studied in multi-resonant dielectric objects in microwave waveguides and as ‘dark state lasers.

2.1.3 Quasi-BICs

Quasi-BICs are a metastable state that decays over a very long-time scale and appears to be a bound state in space. The Q-BIC emerges when the system has an excited discrete state coupled to two overlapping energy bands with divergent singularities in the density of states at the band edges. If the excited state were coupled to only one energy band, a bound state would appear just outside the edge. This would-be bound state is then slightly destabilized by the second energy band, forming a Q-BIC state. If the Q-BIC has an extremely small decay rate the Q-BIC may behave as if it were a bound state even on relatively large time scales [23]. Since Quasi-BICs are known to have small decay rates experimentally, due to noise or structure, the Quasi-BIC state will behave essentially as the BIC under actual experimental conditions, thus, it may be easier to prepare Q-BIC in the experiment. There are two basic types of Q-BICs; stationary Q-BICs states that are characterized by real energies and Schrödinger wave functions that are everywhere bounded, and resonant states having complex energies. Q-BICs have characteristics unlike the other BICs that the perturbation weakly alters the mode so that it leaks to free space with a scattering rate determined by the magnitude of the perturbation and to a polarization state determined by symmetry [22,24]. However, normal Q-BICs are limited to linear polarizations and a fixed phase response, Overvig et al. show that Fano responses from chiral Q-BICs are not bound to linear polarizations and specific amplitude and phase response at resonance. Their finding enables Fano resonant meta-surfaces that

can shape an impinging wave front with spin selectivity exclusively across a designer bandwidth of choice [22]. Originally, the BIC is invisible to manipulation by probing incident fields also propagating in that continuum, but if the scattering problem is granted an extra dimension by introducing a control parameter, the traces of BICs emerge in the scattering spectrum as narrow Fano features once the control parameter is detuned from the BIC point transforming BIC into a Q-BIC. Results from studies are deeply rooted in symmetries, implying that the concepts behind these generalized Fano resonances are not limited to flat optics applications but can be extended to a wide range of wave-based systems, from acoustics and radio frequencies to quantum photonics. The Q-BIC may be useful to produce a high-energy semiconductor laser because the energy difference between a bound state and a Q-BIC can be much greater than the energy difference between two bound states.

2.1.4 Support by Parameter Tuning

Many papers have discussed the effects of geometry symmetry on the BIC symmetry and how certain metamaterials can affect the symmetries as well, which have each given me a direction to take in this work [8,9,19–21,27–33,10,34–43,12,44,45,13–18]. In recent years, researchers have demonstrated and observed BICs in different systems and the associated phenomena. Papers have also discussed the various classes of symmetry found in BICs and how that pertains to Q-BICs structures as well [36]. The notion that BICs can be induced by parameter tuning of the structure, merging of BICs, or manipulating the symmetry of the system is explored to discuss the characteristics and implications [9,11,17,26,36,44,46]. A unique property for resonant cavities is that the two

resonators interact strongly through radiation even when they are far apart. The same principle applies when a single resonant structure is next to a perfectly reflecting boundary, such as a hard wall, or a photonic crystal. A single resonance can also evolve into a BIC when enough parameters are tuned, the single resonance itself can be thought of as arising from two (or more) sets of waves, and the radiation of the constituting waves can be tuned to cancel each other. When the photonic crystal slab has symmetry, up-down mirror symmetry and time-reversal symmetry, the number of radiation channels is reduced. When the number of radiation channels is small, tuning the parameters of the system may be enough to completely suppress radiation into all channels. In many cases, this suppression can be interpreted as an interference effect in which two or more radiating components cancel each other [9]. The resonance turns into a bound state, as shown by the diverging radiative quality factor, which can be determined through the reflectivity spectrum. Such BICs also exist in a linear periodic array of rectangles, cylinders, or spheres as previously mentioned. Single-resonance BICs can also exist in non-periodic structures, as shown theoretically in acoustic and water waveguides with an obstacle, in quantum waveguides and mechanical resonators, and in optics for a low-index waveguide [2,5,6,9]. Although these BICs are not guaranteed to exist by symmetry, when they do exist, they are robust to small changes in the system parameters, and their generation, evolution and annihilation follow strict rules that can be understood through the concept of topological charges. These BICs can be described as ‘protected’ and are known to exist generically if the system parameters be varied over a sufficient range [9]. Topological properties seen for BICs are all-encompassing that they protect each BIC from certain parameters. Photonic EEs supported by periodic systems have been shown

to possess topological features in the form of a polarization singularity. Sakotic et al. have shown that by creating and annihilating singularities, they show that they must obey charge conservation, and provide versatile control of amplitude, phase, and polarization in reflection, with potential applications for polarization control and sensing [12]. Topological characteristics over BICs are characterized by an integer winding number and appear as phase vortices of the complex reflection coefficient. They show that the proposed system supports symmetry-protected and accidental BICs. The topological nature of BICs has kickstarted several research efforts, exploring the merging of BICs to produce even more confined resonances in realistic systems. All real systems have losses, whereas BICs in photonic crystals remain topologically protected if spatial symmetries are not broken. Although photonic crystals have more degrees of freedom to control the topological properties of EEs scattering which offer more versatile control. Other papers discuss the topological properties of BICs in acoustic resonators that describe a synergic effort of theoretical design and experimental verification of super-BICs in a coupled acoustic resonator system arising from the merged BICs. Unlike previous works where BICs arise by periodic structures this is by geometry parameters [19]. Huang et al. also unveiled the general rules of finding out such kinds of supercavity resonances, which could be rigorously correlated to the Friedrich–Wintgen BIC in an entire rectangular resonator with two ports connecting to waveguide. A crucial part of this work is that the aim is to enhance the BIC by merging BICs from a coupled resonator that is not a periodic structure, a similar objective in my work, however with a single resonator.

2.1.5 Metamaterial Influences

Studies have demonstrated that a new generic mechanism to realize bound states in the continuum that exist by first principles free of other resonances and are robust upon parameter tuning. They use a hydrodynamic fluid approach to generate new types of photonic BICs in metamaterials. With this they demonstrate photonic bound states in the continuum in double-net metamaterials. The BICs formed in double-net metamaterials are immune to global symmetry breaking and are only prone to perturbations in the individual networks. They exist within a broad spectral range free of non-BIC resonances and their frequency spacing can be freely tuned by the thickness of the structure. The metamaterial yields an analytical solution with a new type of band which gives rise to photonic bound states in the continuum that are robust even against strong geometrical perturbations and symmetry breakings [15]. All zero-index phenomena can be viewed through the lens of the effective wavelength: as the index approaches zero, waves stretch out toward infinity, and loses its meaning as electric and magnetic fields fill the space uniformly. However, existing demonstrations of integrated ZIM are only suitable for relatively small length scales, due to absorption during propagation. The absorption stems from ohmic loss in the integrated metal waveguides which limit the size of metamaterial devices to tens of microns. Peng et al. discussed in their review that near zero refractive index photonics also enables wave phenomena, such as tunnelling and geometry-invariant eigenmodes, which are exclusive to structures with near-zero parameters [17]. They also propose the light intensity may act as a tuning parameter in nonlinear materials, which may enable robust BICs, tunable channel dropping, light storage and release [17]. Another experiment induced BICs with a zero-index metamaterial (ZIM) to

observe the effects on the BIC present. Zhou et al. found that robust BICs exist and are protected from the disordered distribution of multiple objects inside the ZIM host by its physical symmetries rather than geometrical ones. Regardless of the objects' external shapes and material parameters in the ZIM host, they find that using a certain number of doping objects enables higher-order BICs which was also observed in my work. The existence of geometric-symmetry-free BICs, exist independently on the shape, position, and filling material of the objects is shown. The ZIM causes the total magnetic flux to be nonzero, however in our study to protect symmetries, ZIM is not necessary [10]. Meta-surfaces also have an impact on BICs as they are the planar subwavelength period arrays in which only the zero-order reflection or transmission is permitted. Restricting the radiation channels only to the observable ones, the resonant mode confinement can be infinitely extended by tuning the structural parameters or by the symmetry protection. The meta-surfaces comprise unique architectures in 2D periodic geometry that aids for engineering the optical properties with exotic outcomes due to its low absorption losses strong light–matter interaction through Mie scattering allowing magnetic responses ultimately arising from active dipole radiation [38]. The subwavelength feature are attainable via the current state of the arts in photonics, plasmonics, and meta-materials have promoted attention due to its achievable Q-factors to boost efficient nanoscale activities in contrast to other resonant leaky modes [38]. The last few years have witnessed an unprecedented use of dielectrics in optical metamaterials based on high-index dielectric materials that have strongly emerged as an alternative approach to disrupt the lossy metal-based subwavelength photonics. Dielectric cylinder resonators were theoretically proposed by Richtmyer in 1939 [45]. However, beyond the microwave

frequencies, metals show considerable Ohmic loss, which created the need for all-dielectric resonator platform with the promise to offer low-loss meta optics and photonics. The structures with high Q-factors offer a new route for strong localization of electromagnetic energy in near fields that allow ultrasensitive sensors and other optical devices. Dielectric meta-surfaces can focus electromagnetic waves, generate structured beams and vortices, enhance local fields for advanced sensing, and provide novel functionalities for classical and quantum technologies. Here, Han et al. proposes a BIC-driven terahertz meta-surface with dynamic control of high-Q silicon super-cavities that are reconfigurable at a nanosecond timescale. They employ the physics of BICs for achieving high Q factors in terahertz dielectric meta-surfaces and realize an all-dielectric, active super-cavity that can be dynamically switched at an ultrafast timescale. We employ terahertz (THz) meta-surfaces made up of silicon that offers optically tunable THz conductivity upon excitation by short optical pulses. As a result, the photoconductivity of semiconductors provides a unique approach for the dynamic control of high-Q THz resonances. This approach opens broad views for designing active metamaterials and photonic devices toward filling the THz gap. Thus, a small variation of parameters turns BICs into a leaky mode with extremely high Q factor, which is also known as super-cavity mode. Thus, in most practical devices, all possible BICs turn to super-cavity modes with high Q-factors. In addition, the resonance BICs are affected by the geometrical parameters, in contrast to the symmetry protected BICs, which does not depend on the structural geometry. Furthermore, the inevitable structural imperfectness due to the fabrication process could also break the spatial symmetry of the meta-surface and convert perfect BICs into super-cavity modes with a finite Q-factor or Quasi-BICs.

Findings open a novel avenue, but not limited to, an active control of all-dielectric BIC based meta-surfaces that would enable design of active THz on-chip, ultrafast, low-loss components, and devices such as efficient modulators, filters, and biosensors [44]. The metamaterial allowing for the generation of more BICs robust to geometry changes meaning that selectivity and control can be to the manufacturer.

2.2 Bound States Applications

The applications for BICs in many different regimes are plentiful and rapidly growing with each finding. Over the years, researchers have demonstrated and observed BICs in different systems and the associated phenomena [8,9,19–22,28–32,34,11,35,37–45,12,46–48,13–18]. Hwang et al. addressed the challenge of limited performances of finite-size cavities and studied ways to enhance the strength of nanophotonic devices [29]. To accomplish this, Hwang et al. implemented merging the SP BIC and accidental BICs to demonstrate an efficient laser with a low threshold, high Q-factor, reduced losses, and within a smaller cavity [29]. By merging the BICs in the specific sized periodic photonic structure, the laser has a lower threshold and increased Q-factor. Many previous papers are assumed to be at infinity because it is critical to use a finite structure with a small footprint due to the limited spot size in optical or electrical pumping. They demonstrate efficient lasing in a finite periodic photonic structure for three different regimes using one design: the symmetry-protected BIC laser, accidental BIC laser, and the super-BIC laser which is a combination of the first two BIC lasers. They show lasing action from small-scale dielectric photonic crystal slabs operating in the super-BIC regime. Further analysis shows that in the vicinity of the super-BIC mode

the finite-size cavity can possess a high radiative Q factor, in contrast to the other BIC modes. Findings will pave the way to significantly reduced optical losses in active nanophotonic structures with a finite size and the development of an ultralow-threshold light source for photonic integrated circuits. Further applications of surface-emitting lasers are currently being extended to various low-power fields including communications and interconnections. Studies into applications for bound states and lasers are constantly advancing as further aims in light-matter interaction would be to control strength, directioning, and structures to support these modes. Retracking to the symmetry-protection study Van Hoof et al. they also found that the arrangement of these structures in a photonic lattice can influence their radiation properties to enhance the scattering in certain directions [31]. Another work proposed by Tung Ha had a focus to use dielectric optical antennas that are useful for strong directionality that are straightforward to fabricate and utilize BIC confinement to control directionality. Tung Ha et al. refer to directional lasing the study found that breaking the BIC to form a leaky resonance can aid in controlling the direction of the emitted light with a higher Q-factor, becoming a Q-BIC that can be tuned [37]. Tuning the geometry of the antenna and gain spectrum, the direction and wavelength of the laser can be determined. Results of this work were sourced from an infinitely large system; however, the same characteristics are seen in smaller systems which is beneficial for semiconductor antennas [37]. Also, higher-order multipole resonances can also be used to generate BIC modes in this scheme, provided the symmetry protection is preserved. The avoided crossing in BICs can also be used in real-world applications by understanding the phase matching to use constructive interference to create Q-BICs. A paper by Lee et al. shows that the avoided

crossings in photonic lattices with asymmetric cladding layers support only Q-BICs with a finite value of Q factor, whereas the avoided crossings with symmetric cladding structures support ideal BICs with infinite Q factor. When two guided-mode resonances are coupled, photonic band gaps arise by avoided crossings and BICs appearing in photonic band structures without the fine tuning of structural parameters. This work further shows that depending on the structure it can affect the lifetime and type of BIC supported.

An experiment by Longhi et al. shows that the that the mechanism of light transfer relies on destructive interference and on the existence of a photonic dark state. They found that using a femtosecond laser waveguide structure the transfer efficiency peaks at 87% [34]. A strong reduction in the transfer efficiency is observed when the photonic structure does not support a trapped state in the continuum can indicate the major role played by the destructive Fano-like interference in the transfer process [34]. In this case, if there was an optical BIC present its possible that the transfer efficiency would be able to support it, but since destructive interference implies FW would not be supported but maybe SP BICs will.

Another beneficial impact is efficient optical modulators to quantum-confined structures offering sensitive control over injection of charge carriers and experiments with cold atoms and matter waves [8,12]. By injecting charge carriers, conservation is demonstrated by charge annihilation, tuning the radiation helps to control features and motion of charges. As previously mentioned, that the need for all-dielectric resonator platform with the promise to offer low-loss meta optics and photonics, a study by Marinica et al. shows that if one is controlling the BIC means you can use in

subwavelength arrays, so numerous domains of nano-photonics, including, but not limited to, biological sensing, Raman scattering, multifunctional on-chip lasers are enhanced [21,26,32,37,44,48]. The last few years have witnessed an unprecedented use of dielectrics in optical metamaterials based on high-index dielectric materials that have strongly emerged as an alternative approach to disrupt the lossy metal-based subwavelength photonics. The structures with high Q factors offer a new route for strong localization of electromagnetic energy in near fields that allow ultrasensitive sensors and other optical devices. The double net metamaterial discussed earlier is another material to help excite BICs in structures. The metamaterial yields an analytical solution with a new type of band which gives rise to photonic bound states in the continuum that are robust even against strong geometrical perturbations and symmetry breakings. This metamaterial is made out of a hydrodynamic fluid, however, the effects are similar to that of the ZIM medium [15,17]. Not as intrinsic as ZIM, however the dynamic fluid is in the surrounding area which makes it practical for many applications in water and acoustic waves [1,3,6,16]. A ZIM medium as we know helps to nullify the limitations in dielectrics and symmetries are left untouched when interacting with a ZIM. In a photonic structure, near-zero refractive index exhibits very distinctive features in basic light-matter interaction processes including the propagation, scattering, emission and confinement of light [17]. Nonlinear optics, flexible photonics, quantum information processing and heat management seem to be some of the most promising areas arising. However, their technological impact will be determined by our ability to develop high-quality and low-loss structures with near-zero parameters.

More acoustic demonstrations are shown by Huang et al. that a specific open resonator can support multiple BICs and furthermore, the magnitude of Q-factor increases as well [16]. Huang et al also proposed in another paper using the topological characteristics of the BIC that it is possible to merge BICs to enhance the Q-factor like mentioned in the previous section [19]. Taking this further, Joseph et al. discuss the topological charge control in BIC by tailoring the opto-geometrical parameters and incident illumination sources explore the generation of vortex beam and lasing sources [38]. Increasing Q-factor can be useful for constructing high-performance acoustic devices, such as acoustic filters, acoustic sensors, and acoustic lasers. In optical BICs, increasing the Q-factor can increase the interaction time between light and matter by orders of magnitude [9]

As previously mentioned, Han et al. employ the physics of BICs for high Q-factors in THz dielectric meta-surfaces, however, since small variation of parameters turns BICs into a leaky mode with extremely high Q-factor then in most practical devices, all possible BICs turn to super-cavity modes with high Q-factors [45]. The inevitable structural imperfectness due to the fabrication process could also break the spatial symmetry of the meta-surface and convert perfect BICs into super-cavity modes with a finite Q-factor. Applications include biosensing, modulators and filters. Another study to tie in with dielectric resonators is one by Azzam et al. discussing combining different physical mechanisms in a single dielectric array without intricate designs [40]. Using the framework to manipulate the electric and magnetic dipoles in dielectric resonators, they explore multi-mode lasing. For this, they show that the BIC-assisted mode engineering in arrays of dielectric nano-resonators and show multi-wavelength

directional lasing. Two-and three-mode lasers have been demonstrated experimentally, showing the potential for this type of structure to support controllable multi-wavelength on-chip micro-lasers [40].

The structure with a BIC can be a perfect filter or waveguide at resonance frequency [32]. The use of resonant structures may improve substantially both the performance and efficiency of subwavelength integrated photonics actively discussed in the current literature. More applications include parallel biosensors, compact spectral splitting solar cells, low-threshold nano-lasers, single-photon sources, and surface-enhanced sensors. Currently being expanded with high index medias, this platform can also be transferred to terahertz, infrared, and optics as we have seen [18,44,48].

Literature currently points in the direction of controlling these states and enhancing the Q-factor in practical cases. The way that Q-factor was estimated was based on positive and negative dipoles. Vučković et al. presented a method for estimating the factor of a mode and its radiation loss from the known Fourier transform of the near-field distribution. By applying this approach to high structures that were proposed recently, it has been proven that the optimization of the factor of the dipole defect mode [42]. Designs for specific diffraction gratings have been demonstrated by Monticone et al. [13]. They establish simple and general design guidelines to obtain trapped states in realistic grating structures, and further validate their theoretical predictions with numerical simulations. They show that such trapped states resulting in a mode completely decoupled from free-space radiation, which manifests itself in the diffraction spectrum as a Fano resonance with diverging Q-factor [13]. Another design idea presented by Bulgakov et al. is a structure that contains a periodic structure of dielectric rods inside the

cavity. Results from the paper detail the effects of dielectric rods in a photonic crystal, singular BICs were not realized however the Fano resonance width became narrow which still signifies a BIC [14]. Applications from generalized Fano resonances are not limited to flat optics applications but can be extended to a wide range of wave-based systems, from acoustics and radio frequencies to quantum photonics [22]. Photonic structures are known to support various BICs, and one study aims to control optical beams by using multiple beams and a photonic crystal slab that supports a SP BIC [28]. Other structure designs implement a 3D photonic crystal that symmetry bandgaps can be realized in low-index systems but also that the benefits of environmental design require only a single layer of the environment on both sides of the system, implications include enabling multi-frequency and multi–wave vector in technology [47]. On the other side of using low-index dielectric material, one can use high-index and it's found that on an integrated platform that takes away the need to specifically pattern the micro/nano structures [43]. The Fano concept may also be extended to other applications such as photodetectors and electro-optic modulators, with the prospect of largely reducing the energy consumption and increasing the bandwidth of on-chip integrated photonic interconnects [39].

The applications for BICs are quite limitless if they regard wave propagation, however the specific ways to tune BICs or structures for the best quality is left to interpretation on what parameters are necessary.

Chapter 3

Approach

To develop an overall approach for the addressing the scope of the research work presented in this thesis, we briefly revisit the objectives of this project:

1. Identify characteristics and critical factors in cavity structures and design a structure that support embedded eigenmodes (EE);
2. Expand the structure to study dependencies to dimensions along with embedded scatterers;
3. Utilize numerical simulations and established theories in comparisons to verify symmetry parameters.

The design that is developed in this thesis, which is composed of an open cavity resonator is described in Section 3.1. The evaluation methods for determining the effectiveness of the approach are described in Section 3.2. A previously suggested open cavity resonator structure from "Sound trapping in an open resonator" [16] is adapted along with the Coupled-Mode theory and Fano resonance calculations [4,5,9,30] for the specific purposes of the design and information processing described in this thesis. The implementation results are presented and discussed in the following chapter.

3.1 Cavity Design

Previous works use many different types of cavity structures and configurations to observe, and study bound states in their various forms. As mentioned in prior chapters, these include open and closed resonators with defects, cylindrical or

spherical cavities. [10,32]. The specific geometry structure has a crucial impact on the symmetry of the BIC supported. Here we consider a rectangular resonator for microwave propagation in the GHz regime. Figure 1(a) depicts the proposed structure in this study which contains a 2D open resonator attached to a waveguide. Each of the boundary walls in the structure are perfect electrical conductors (PECs) with the ends of the waveguide being the input and output ports, respectively. The original geometry dimensions start with the waveguide's width w_w = 20mm and waveguide's height w_h = 120mm. The connecting neck width n_w = 30mm and neck height n_h = 20mm. The cavity's width c_w = 86mm and the cavity's height c_h = 64mm. Next, dielectric scatters are implemented into the structure to observe the effects on the BICs. The dielectric rods used in this study have a radius r_d of 10mm with the dielectric inside being Teflon and are positioned symmetrically about the horizontal axis in the cavity. The dielectric rod is wrapped in a thin aluminum layer with relative permeability and permittivity is 1, the electrical conductivity is 3.774e7 S/m [10]. The properties of Teflon are relative permeability is 1, relative permittivity is 2.1 and electrical conductivity is 10^-25 S/m. Previously dielectric rods have been proposed to manipulate BICs in different structures [10,18]. These dielectric rods alter the field distribution by interacting with the structures or causing scattering effects. On the other hand, it is shown that for a zero-index material (ZIM), the scatters would not affect the BICs because in a ZIM filled cavity the BICs are independent from the dielectric rods [10,17]. In this work, we are focusing on the interactions between the scatters and the host resonator. The SP Q-BICs we want to examine and influence in the resonator is shown in Fig. 1(b) & 1(c). When the dielectric scatters are introduced, the field distribution inside the cavity is altered. For example, the

magnetic field has a larger intensity near the rods. Simulations show that location of the dielectrics is crucial as the field distorts in the region. On the other hand, the degree of suppression depends on the location of the rods. It should be noted that only select cases of dielectrics in the top are shown, identical effects are seen in their bottom counterparts for future illustrations.

Figure 1

Resonator Structure and BICs of An Open Microwave Resonator

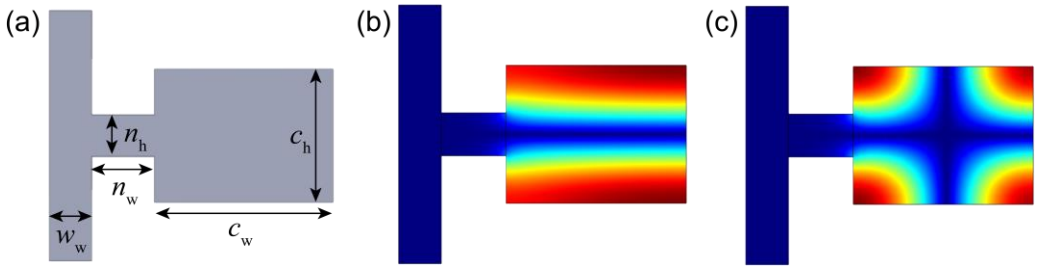

Note. **(a)** Structural configuration of the resonator. **(b)** Magnetic field distribution of the 12-mode and **(c)** 22-mode inside the structure without dielectric rods.

3.2 Method Evaluation

A plane wave solution to the wave equation can be found in an electric field with only an x component and no variation in the x and y directions [49]. The reduced Helmholtz equation considers propagation in the z direction. Theoretically, the resonator-waveguide structure can be described by the scalar wave function $\psi_m(x,y)$ which describes the H_z component which obeys the Helmholtz equation: $\widehat{H}\psi_m(x,y) = (\frac{\omega_m^2}{c^2})\psi_m(x,y)$, where $\widehat{H} = \nabla^2 + [n^2(x,y)+1]\omega_m^2/c^2$ is the Hamiltonian, ω is the frequency and c is the light speed [10]. To estimate the quality factor of the cavity, the reflection coefficient is

calculated. Because the energy in the cavity will reflect not transmit, this helps verify the existence of the BICs by measuring the reflection between the ports. When an open electromagnetic structure (e.g., an open cavity, or waveguide) is externally illuminated, the presence of highly confined modes often manifests itself in the form of narrow asymmetric resonances, Fano resonances, in the reflection, transmission or scattering spectra [13]. Each structure has a Fano resonance, with an asymmetric line-shape and smooth curve to each. To verify the existence of a bound state is to check the Fano resonance peaks which display the two scattering amplitudes: the continuum of states and the resonant state [16,21,46]. If the Q-factor plummeted in a structure, the asymmetry of the Fano resonance can still indicate a BIC. The use of the coupled-mode theory (CMT) is employed in many works as an accurate method to evaluating the Fano resonance-like parameters in a coupled waveguide system [14,18–20,22,47]. We employ the CMT method to plot the Fano curve of these modes in Fig 2(a) & 2(b). Control of the Fanolike parameters has also been proposed to have selectivity over the transmission dynamics by two structures, one structure relies on controlling the amplitude of one of the paths and the other uses symmetry breaking [39]. When observing the Fano resonance, the step size of the frequency is important, because as the size gets smaller you can infer that the lineshape has a very narrow width. This further upholds the high Q-factor and its sharpness in the Fano peak. In the meantime, numerical simulations based on finite element method using COMSOL Multiphysics are carried out to validate the theoretical model. In COMSOL, one port is used as the input and the reflection coefficient is recorded at that port. An eigenvalue study is also carried out to obtain the quality factor of the cavity, which is done by relating the

real and imaginary parts of the eigenvalues. The real parts respond to the position of the resonances while their imaginary parts respond to the half resonant widths [10].

$$R = \frac{(\omega-\omega_0)^2 \cos^2\theta+\gamma^2 \sin^2\theta \mp 2 \sin\theta \cos\theta(\omega-\omega_0)\gamma}{(\omega-\omega_0)^2+\gamma^2} \quad (1)$$

In Equation 1. we have ω_0 as the resonance frequency, γ is the decay rate, and θ is the phase angle of the eigenfrequency. The reflection coefficient can be obtained by calculating the resonance frequency and decay rate obtained from the eigenvalue study for EM waves in COMSOL. The resonance frequency is the same as the eigenfrequency of the BIC that is observed, related to the Q-factor which COMSOL calculates from the eigenvalues. The imaginary part of the eigenfrequency is where the radiative decay rate is measured. It should be noted using the Q-factor equation you can also find the decay rate for further verifying COMSOL's results, both are equally viable for calculations. The reflection coefficients are also compared with results obtained by COMSOL using structures whose geometry is outlined in Fig. 1(a). The underlying concept behind the emergence BICs is because the radiation at the neck cancels out due to the symmetric field distributions. However, due to the geometry of the structure we lose the symmetry and idealness of the BIC to form a Q-BIC. To observe this, cutline plots are taken along the neck connecting to the waveguide to measure the magnetic field. A cutline plot is shown in Fig. 2(c) where it is found that the magnetic field at the neck exhibits symmetric distributions meaning it maintains a high Q-factor.

Figure 2

Coupled Mode Theory and Neck Symmetry

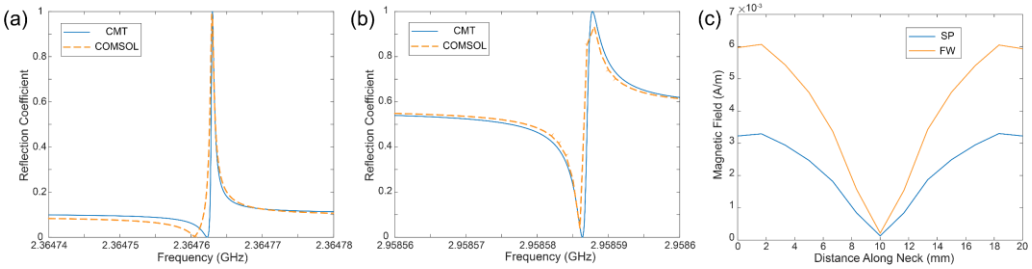

Note. **(a)** CMT and COMSOL for the 12-mode. **(b)** CMT and COMSOL for the 22-mode. **(c)** A plot to measure the magnetic field at the neck of the connector to find symmetry.

Chapter 4

Results

The original Q-BICs our structure supported consisted of multiple SP modes. Figure 1 depicts modes at specific eigenfrequencies. These were found to mimic quasi-bound states by their stability in the fields and high Q-factors of 5.1886e6 and 2.086e6, respectively.

4.1 Geometry Change Effect

To begin with, we first alter the cavity's width and height to study the dependence of quality factor of the Q-BICs to the geometrical parameters of the cavity, shown in Fig. 3. We are varying one parameter while fixing the other. With the previous pair of Q-BICs, we further tune the geometry to study the manipulation. By incrementally increasing the cavity, the Q-factor of the bound states increases for both modes. Figure 3(a) & 3(b) shows an increase to the cavity's width and height, which results in an increase in the Q-factor of the system for both modes at a similar rate. This shows that increasing the cavity can produce higher Q-factors, and from this it is possible that the introduction of dielectric scatters can help separate these Q-BIC modes by suppressing one. A noticeable trend is that the 12-mode is more robust to an increase in the width than the 22-mode. A trend we found in our structure, the larger the neck height led to a decrease in the Q-factor. Symmetry itself in the Q-BICs is seen to be destroyed as the energy in the cavity leaks back out to the neck. Fig. 3(c) & 3(d) shows the extension of the neck height and width. Symmetry in the 12-mode is maintained, not the 22-mode, however the Q-factor increase is negligible. Increasing the neck width does not lead to

altering the field distribution, also shows that the neck's width will not destroy the symmetry in the cavity. A study on resonators discusses the importance of symmetry of the entire structure and certain parameters that can affect the perturbation, thus manipulating the Q-factor [16]. Similar trends were found in our structure, the larger the neck height led to a decrease in the Q-factor. With both symmetry itself in the Q-BICs is seen to be destroyed as the energy in the cavity leaks back out to the neck.

Figure 3

Effects to Q-factor by Extending the Cavity in Width and Height Separately

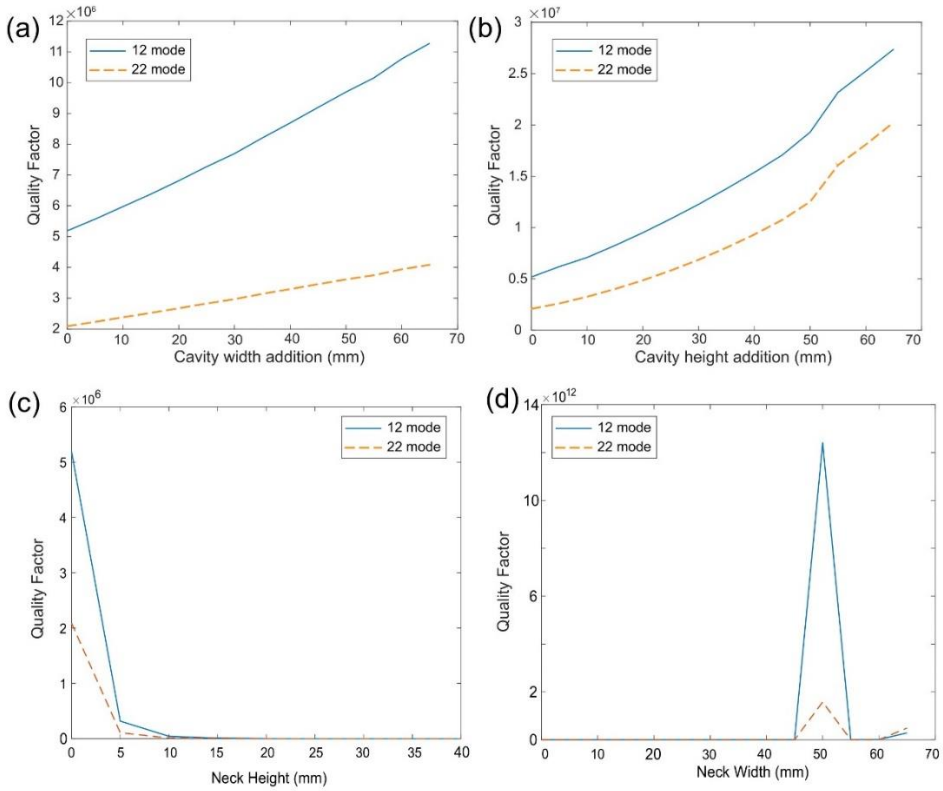

Note. **(a)** Shows the effects on the Q-factor by extending the ca_w width. **(b)** Shows the effects on the Q-factor by extending the ca_h height. **(c)** The effects on quality factor by extending n_h height. **(d)** The effects on quality factor by extending n_w width.

On the other hand, the frequency of both 12-and 22-modes decreases as the cavity width increases, as evidenced by the Fano resonances shown in Fig. 4. A steady increase in the reflection coefficient as the width increases is demonstrated. This is expected as size of the cavity gets larger when its width is increased. The Fano curves increasing means that a sharp asymmetric peak in the Q-factor is reached at lower eigenfrequencies and in our case, higher Q-factors.

Figure 4

Fano Resonance Plots of Various Cavity Widths

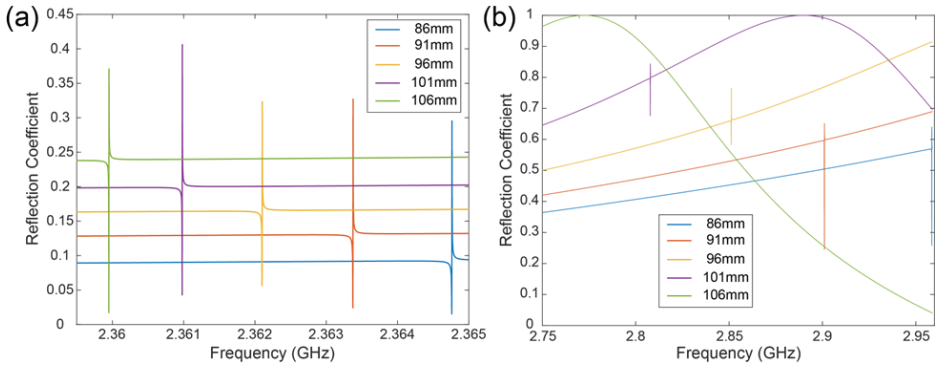

Note. **(a)** Fano Resonance of the 12-mode. **(b)** Fano Resonance of the 22-mode.

4.1.1 Dielectric Scattering Rods

When the dielectric scatters are introduced, the field distribution inside the cavity is altered. For example, the magnetic field has a larger intensity near the rods. Simulations show that location of the dielectrics is crucial as the field distorts in the region. On the other hand, the degree of suppression relates on the location of the rods, due to symmetry. It should be noted that Fig. 5 shows only select cases of dielectrics. The top is shown because identical effects are seen in their bottom counterparts. Dielectrics are known to have properties that can induce field enhancements and stronger magnetic field confinement in specific "hot spots," improving the values of the Q-factor [11,14,44], which we see in Fig. 5. When further away the 12-mode maintains a higher Q-factor when the rods are located further away from the neck, depicted in Fig. 5(b). The 22-mode has a higher Q-factor when the rods are located closer to the neck, shown in Fig. 5(c). Regions of the field that were present are now diminished, clustering at the dielectric. In all these cases, a dramatic decrease in term of the Q-factor is

observed, which can be explained by the fact that the locations of the scatters defy the original symmetry of the Q-BIC modes, and the scattering of the rods causes higher radiation and hence a lower Q-factor. We see that the Fano resonance makes a close approximation between numerical simulations and the CMT, shown in Fig. 5(e) & 5(h), specifically for the cavity with the dielectric to the right. The structure's Q-BICs were higher, and the 12-mode was more robust compared to its left counterpart. The deviation helps explain the loss of Q-factor in the structure. This is also confirmed by the cutline plot of the field Fig. 5(g) & 5(h) where an asymmetric field distribution at the neck is observed. Meaning for these Q-BICs to not yield a symmetric line shape, but maintain a high Q-factor, energy is perceived to be leaking out.

Figure 5

COMSOL Depictions of the Magnetic Field Modes Inside the Structure with Dielectric Rods

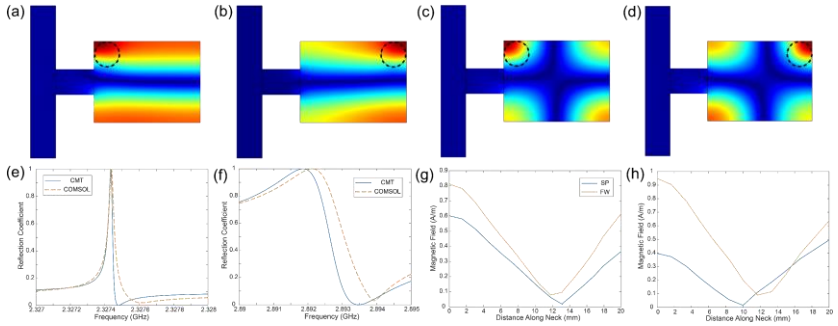

Note. **(a)** & **(c)** BIC modes of the structure with a dielectric in the top left, 12-and 22-modes, respectively. **(b)** & **(d)** BIC modes of the structure with a dielectric in the top right, 12-and 22-modes, respectively. **(e)** Plot for RT 12-mode Fano Res. **(f)** Plot for RT 22-mode Fano Res. **(g)** Plot for LT Cut Line **(h)** Plot for RT Cut Line in Figure 5.

4.1.2 Symmetric Dielectric Scatters

To illustrate the relation between the symmetry conditions of the scatters and the original Q-BIC modes, we further add another dielectric rod symmetrically to the bottom of the cavity so that the two scatters are symmetric with respect to the horizontal axis. In Fig. 6 we have the dielectric rods on the leftmost, center, and rightmost of the cavity for the 12-and 22-modes, respectively. These regions are where symmetry may be the strongest for specific modes and dielectric location. Distances in the cavity for these, respectively are 0mm, 33mm, and 66mm.

Figure 6

COMSOL Depictions of the Magnetic Field Modes Inside the Structure with Dielectric Rods

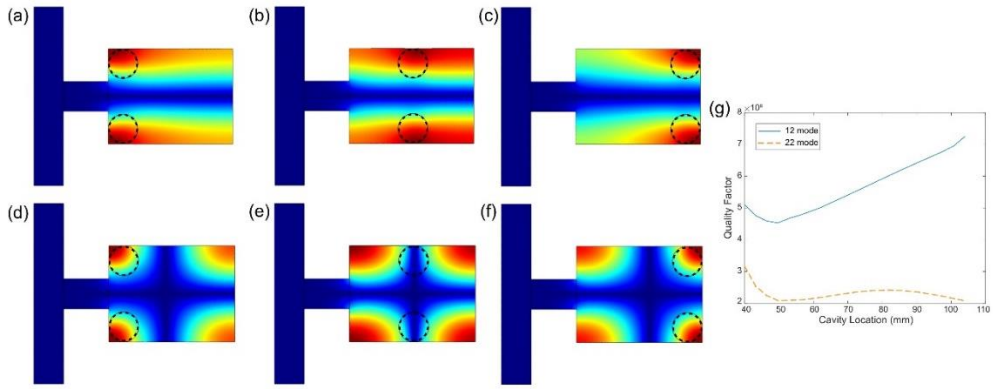

Note. **(a)** & **(d)** Magnetic field of the 12-and 22-modes to the left. **(b)** & **(e)** Magnetic field of the 12-and 22-modes in the center. **(c)** & **(f)** Magnetic field of the 12-and 22-modes to the right. **(g)** Quality factor trend from the left to the right.

According to the field distribution in Fig. 6, the locations are consistent for the symmetry condition of the 12-and 22-modes (e.g., mirror symmetry about the x-axis). The results are shown in Fig. 6(g) where the rods are moved across the cavity. When moving the rods across the cavity we see the Q-factor vary for both the 12-and 22-modes. Dielectric rods placed at the direct center of the cavity yields higher Q-factor values for both BICs. Comparing the Fano resonance at each location, illustrated in Fig. 7 show that numerical simulations and computational methods curves show good agreement, as well as an asymmetric line-shape meaning the energy is not radiating out. The increments in Figure 7 each are in magnitudes of 10^{-7}~ 10^{-8}GHz which shows that there is a narrow linewidth of these curves which shows a high Q-factor.

Figure 7

Fano Resonance Plots of Dual Dielectric Scatters

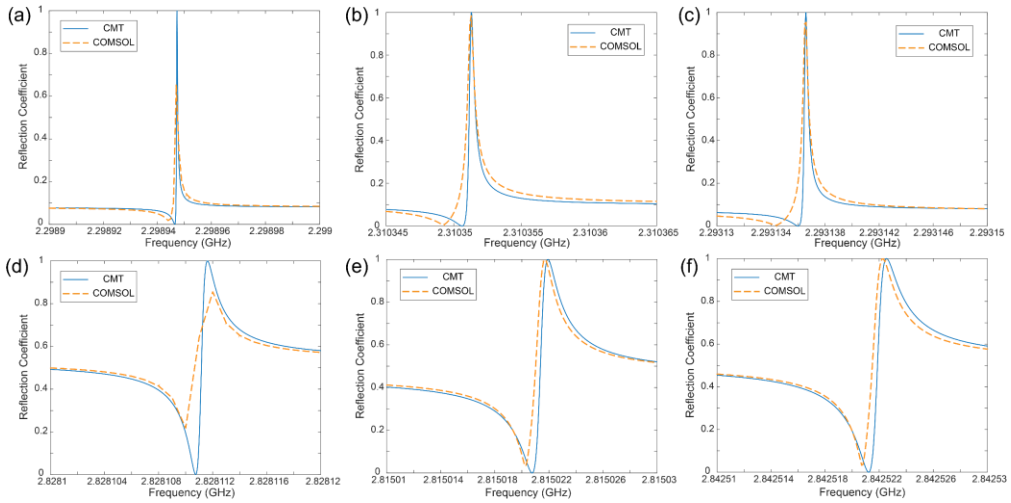

Note. **(a)** & **(d)** Magnetic field symmetry at the neck for dual dielectrics to the left, 12- and 22- respectively. **(b)** & **(e)** Magnetic field symmetry at the neck for dual dielectrics in the center, 12-and 22-. **(c)** & **(f)** Magnetic field symmetry at the neck for dual dielectrics to the right, 12-and 22-.

4.1.3 Asymmetrical Dielectric Scatters

To gain more insight into the behavior of 22-mode, we place the rods asymmetrically in the cavity, in opposite corners of the cavity. Fig. 8 shows that the field itself is distorted for the 12-mode, while the field is symmetrical for the 22-mode, shown in Fig. 8. In previous results, we demonstrated that implementing scatters can influence both modes simultaneously. Also previously mentioned, naturally, the scatters would suppress the modes, which is also the case in Fig. 9.

Figure 8

COMSOL Depictions of the Magnetic Field Modes Inside the Structure with Asymmetric Dielectric Rods

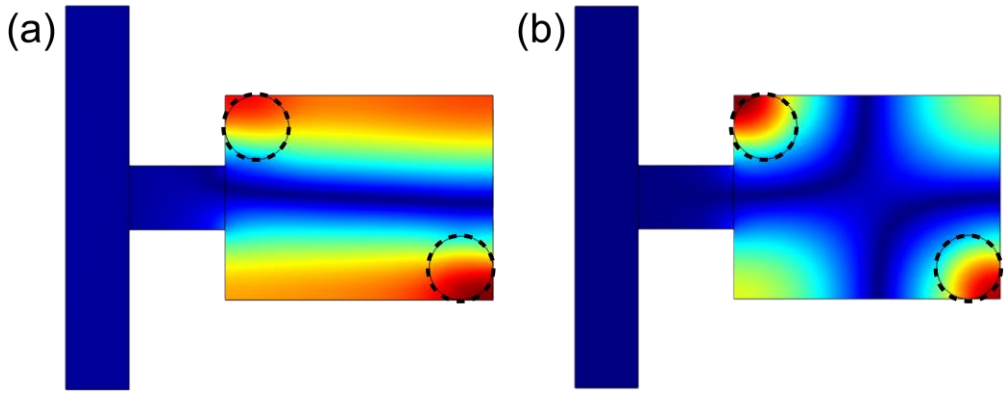

Note. (a) Magnetic field of the 12-mode. (b) Magnetic field of the 22-mode.

However, when the cavity is altered, there are special situations where the Q-BICs are still maintained. We modify the cavity's width and height separately like previously done and we keep the dielectric rods in the corners shown in Fig. 9. It is seen that increasing the cavity height can increase the 12-mode's Q-factor. However, the symmetry of 22-mode is distorted compared to previous findings. In a plot of the Q-factor vs. cavity height, in Fig. 9(a) shown below, the 12-mode has a large increase in quality as the height is increased. The 22-mode drops to magnitudes of 10^3. The 22-mode appears symmetrical, but the Q-factor is seen to only rise minimally as the height increases. Indicators here show that the 22-mode is suppressed.

Figure 9

Results of Scatters Placed Asymmetrically in the Cavity

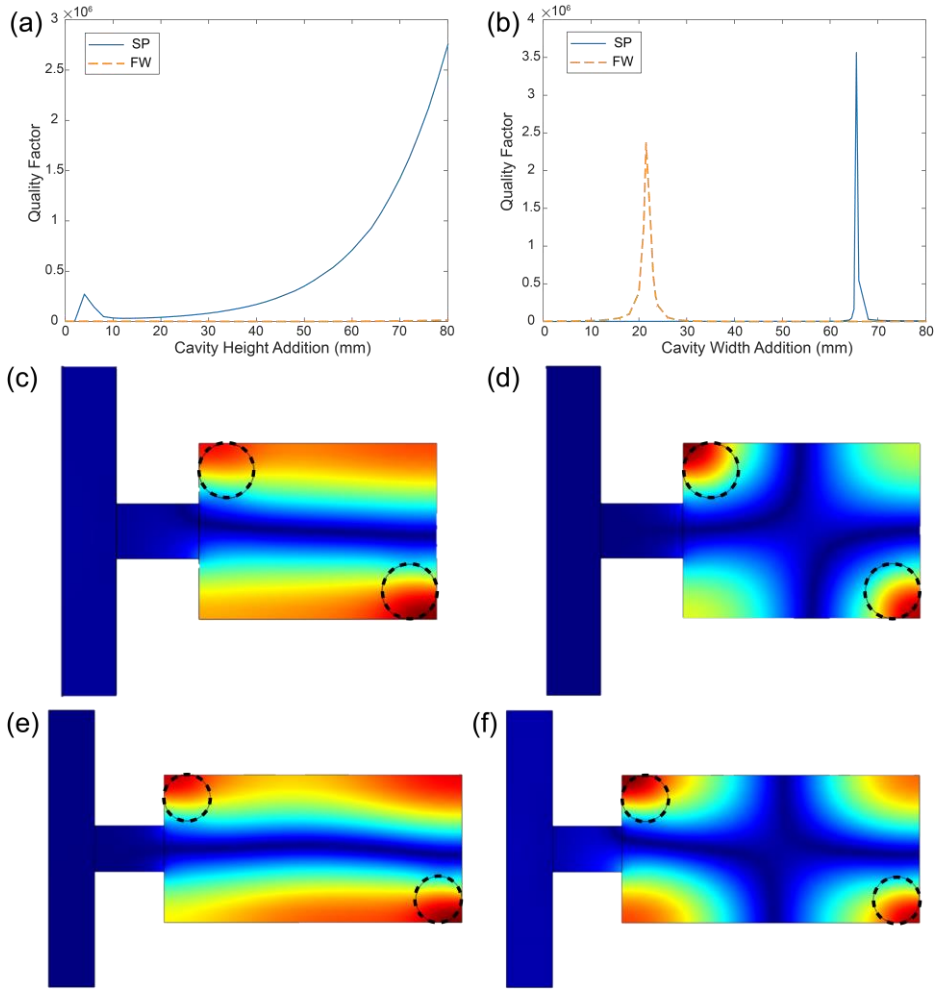

Note. **(a)** Cavity extension in height. **(b)** Cavity extension in the width. **(c)** & **(d)** Magnetic field for c_w of 86.5mm. **(e)** & **(f)** Magnetic field for c_w extension of 128mm.

Figs. 9(a) & 9(b) show a trend in the Q-factors of the Q-BICs by increasing the width. The Q-factor vs cavity width curve reveals that the geometry can be tuned to achieve better Q-factors for the system in specific modes. By extending the c_w, different modes are amplified at specific widths. We see that at 86mm the 22-mode has a higher

Q-factor while the 12-mode plummets. At c_w = 128mm, the 12-mode has a higher Q-factor while the 22-mode is suppressed. At c_w= 114mm both Q-BICs are destroyed. Nevertheless, it is possible to selectively excite eigenmodes by carefully tailoring the dimension of the cavity so that the radiation at the neck is still maintained. Ability to specify which modes to excite and suppress others can be very useful when applying to systems that involve waveguides and resonators. To verify results, the symmetry of the magnetic field is observed at the neck in Fig. 10 where from the cut-line plots we are able to see that symmetry is maintained for specific Q-BIC modes, showing that the radiation is canceled out. Altering the cavity with dielectrics inside makes choosing specific modes in structures become feasible.

Figure 10

Magnetic Field Symmetry Plots for BICs at Separate Widths

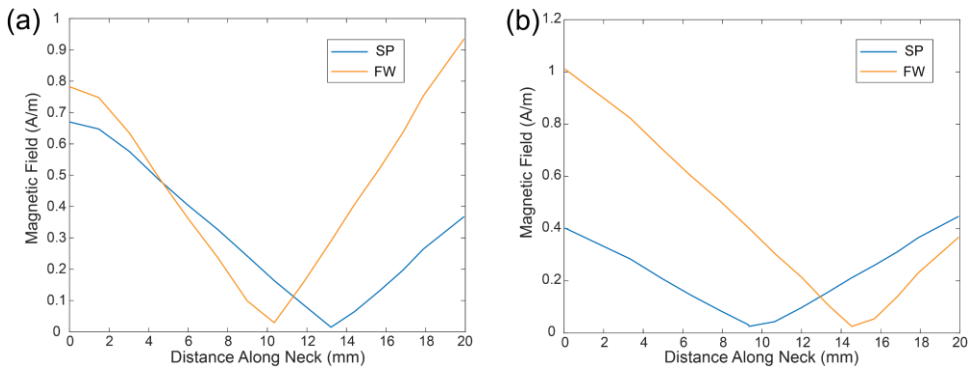

Note. **(a)** Symmetry plot of 12-and 22-modes with dielectrics at 86.5mm. **(b)** Symmetry plot of 12-and 22-modes with dielectrics at 128mm.

4.2 Symmetric Cavity

The eigenmodes demonstrated in the previous section can be supported by a cavity of varying aspect ratio to illustrate the symmetry-protected 12-and 22-modes. However, a way to illustrate the Friedrich-Wintgen mode is made known by making the cavity symmetric on each side, shown in Fig. 11. The structure now supports the SP BICs and FW BIC for further observation. The structure was symmetric about the x-axis and not the y-axis which would not allow the FW BIC to arise because destructive interference was not allowed, however, when the aspect ratio becomes 1 the FW BIC can be studied. With the cavity width being 86mm on each side, we see the different modes, each with high Q-factors. The 12-mode we previously noted is now in magnitudes of 10^7, the 22-mode of 10^6, and the FW mode of 10^5. We cannot change the aspect ratio of the cavity since that will destroy the FW BIC, but we see that making the cavity smaller or larger entirely makes the Q-factor decrease or increase as well.

Figure 11

Friedrich-Wintgen BIC

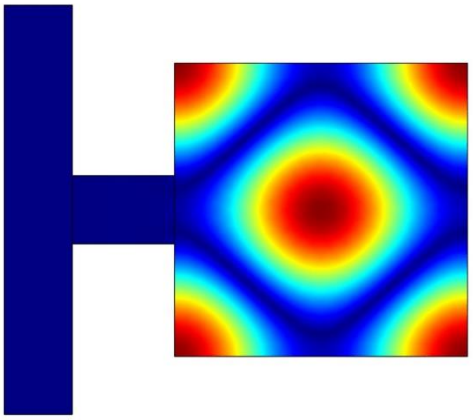

4.2.1 Dielectric Scattering Rods

Unable to alter the cavity's aspect ratio as that would destroy the FW BIC, we add dielectric scattering rods to the structure. Placing the rods in the same way as the prior structure, we see from the Q-factors and field distributions that each of the modes are effectively diminished by the introduction of dielectric rods. There are regions where the rods have a degree of control over the BICs. When we place the dielectrics asymmetrically, we see the FW BIC rise above the 12-and 22-modes, which is in the range of 10^5 compared to $10^3 \sim 10^4$ respectively. When the SP Q-BICs are enhanced, and the FW BIC is suppressed it is from the dielectrics obeying the symmetry of the SP Q-BICs and not the FW BIC. The Fano resonance curve for these configurations display an asymmetric curve to account for the high Q-factor to further show the existence of these BICs. The step size of the Fano resonance is in magnitudes of 10^{-7}which shows that the Q-factor sharply rose for this BIC. The FW BIC Q-factor is in magnitudes of 10^5 which supports this. The magnetic field measured at the neck of the cavity has a symmetric curve demonstrating stability, and in this case, destructive interference. This degree of freedom gives flexibility to the manufacturer that if the structure has strict symmetric demands, the BICs can be tuned with dielectric scatterers for desired results.

Figure 12

Fano Resonance Curve and Magnetic Field Symmetry for FW BIC

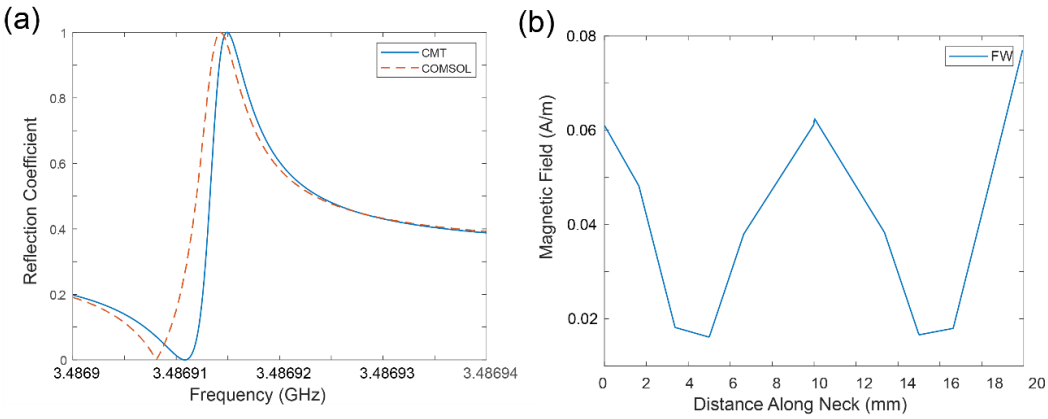

Chapter 5

Conclusions

Theories on BICs can be expanded upon from prior knowledge using theories and calculations from acoustic resonators in relation to EM waves. This study is to discuss known Q-BIC modes and unknown details that surround them. We have presented that Q-BIC modes in structures can be enhanced by specific geometry alterations alone, however the introduction of dielectric scatters can affect these Q-BIC symmetries.

1. Identify characteristics and critical factors in cavity structures and design a structure that support embedded eigenmodes;
2. Expand the structure to study dependencies to dimensions along with embedded scatterers;
3. Utilize numerical simulations and established theories in comparisons to verify symmetry parameters;

The specific contributions outlined in this thesis are:

1. The location of these dielectric scatters is important as in some cases, it can decrease modes by significant magnitudes. However, placing dielectrics in an asymmetric pattern can result in the amplification of certain modes compared to others in the same structure which is directly tied to the goal of manipulating the Q-BICs;
2. Furthermore, by placing these scatters asymmetrically and varying the cavity, there is a degree of control over the excitation of specific modes.

The proposed structure is not the only structure it is seen in, however, using a rectangular resonator provides very conducive results from previous studies. The ability

to tune the geometry to reach higher Q-factors is highly valuable for many applications such as nonlinear enhancement, coherent light generation, sensors, filters, integrated circuits, and many others [12,29,33,37,38,40,41]. Real world applications can be demonstrated in optical physics with photonic structure lasers where SP BICs did not yield high Q-factors [8,11,41,42,44,45,47,12,14,23,29–31,34,40]. Regarding experimental applications, values obtained may not be as accurate as numerical simulations as COMSOL has values set for perfectly ideal conditions which is not the case in practice due to possible loss in the walls, the waveguide, and connector. Let it be noted the CMT findings for the Q-BICs agrees with COMSOL but only to an extent when the rods are introduced. This is because the Q-factor does not span the entire spectrum evenly as COMSOL may seem and loss must be factored in. However, being able to create a design that closely resembles values from ideal conditions back into calculations can lead to further studies with finer results. This thesis attempts to take early steps in manipulating and magnetic fields as whole.

References

[1] E. B. Davies and L. Parnovski, *Trapped Modes in Acoustic Waveguides*, Q. J. Mech. Appl. Math. **51**, (1998).

[2] C. J. Fitzgerald and P. McIver, *Passive Trapped Modes in the Water-Wave Problem for a Floating Structure*, J. Fluid Mech. **657**, 456 (2010).

[3] C. M. Linton and P. McIver, *Embedded Trapped Modes in Water Waves and Acoustics*, Wave Motion **45**, 16 (2007).

[4] P. McIver and M. McIver, *Trapped Modes in an Axisymmetric Water-Wave Problem*, Q. J. Mech. Appl. Math. **50**, 165 (1997).

[5] P. McIver and M. McIver, *Motion Trapping Structures in the Three-Dimensional Water-Wave Problem*, J. Eng. Math. **58**, 67 (2007).

[6] P. J. Cobelli, V. Pagneux, A. Maurel, and P. Petitjeans, *Experimental Study on Water-Wave Trapped Modes*, J. Fluid Mech. **666**, 445 (2011).

[7] J. von Neumann and E. P. Wigner, *Über Merkwürdige Diskrete Eigenwerte*, in *The Collected Works of Eugene Paul Wigner: Part A: The Scientific Papers*, edited by A. S. Wightman (Springer Berlin Heidelberg, Berlin, Heidelberg, 1993), pp. 291–293.

[8] Y. Plotnik, O. Peleg, F. Dreisow, M. Heinrich, S. Nolte, A. Szameit, and M. Segev, *Experimental Observation of Optical Bound States in the Continuum*, Phys. Rev. Lett. **107**, 28 (2011).

[9] C. W. Hsu, B. Zhen, A. D. Stone, J. D. Joannopoulos, and M. Soljacic, *Bound States in the Continuum*, Nat. Rev. Mater. **1**, (2016).

[10] Q. Zhou, Y. Fu, L. Huang, Q. Wu, A. Miroshnichenko, L. Gao, and Y. Xu, *Geometry Symmetry-Free and Higher-Order Optical Bound States in the Continuum*, Nat. Commun. **12**, 1 (2021).

[11] K. Koshelev, G. Favraud, A. Bogdanov, Y. Kivshar, and A. Fratalocchi, *Nonradiating Photonics with Resonant Dielectric Nanostructures*, Nanophotonics **8**, 725 (2019).

[12] Z. Sakotic, A. Krasnok, A. Alú, and N. Jankovic, *Topological Scattering Singularities and Embedded Eigenstates for Polarization Control and Sensing Applications*, Photonics Res. **9**, 1310 (2021).

[13] F. Monticone and A. Alù, *Bound States within the Radiation Continuum in Diffraction Gratings and the Role of Leaky Modes*, New J. Phys. **19**, (2017).

[14] E. N. Bulgakov and A. F. Sadreev, *Bound States in the Continuum in Photonic Waveguides Inspired by Defects*, Phys. Rev. B - Condens. Matter Mater. Phys. **78**, (2008).

[15] W. Wang, A. Günzler, B. D. Wilts, and M. Saba, *Electronic Acoustic Waves and Bound States in the Continuum in Double-Net Metamaterials*, **1**, (2021).

[16] L. Huang, Y. K. Chiang, S. Huang, C. Shen, F. Deng, Y. Cheng, B. Jia, Y. Li, D. A. Powell, and A. E. Miroshnichenko, *Sound Trapping in an Open Resonator*, Nat. Commun. **12**, 1 (2021).

[17] Y. Peng and S. Liao, *Bound States in Continuum and Zero-Index Metamaterials: A Review*, 1 (2020).

[18] T. Lepetit and B. Kanté, *Controlling Multipolar Radiation with Symmetries for Electromagnetic Bound States in the Continuum*, Phys. Rev. B - Condens. Matter Mater. Phys. **90**, (2014).

[19] L. Huang, B. Jia, Y. K. Chiang, S. Huang, C. Shen, F. Deng, T. Yang, D. A. Powell, Y. Li, and A. E. Miroshnichenko, *Topological Supercavity Resonances in the Finite System*, Adv. Sci. **9**, 1 (2022).

[20] A. F. Sadreev, *Interference Traps Waves in an Open System: Bound States in the Continuum*, Reports Prog. Phys. **84**, (2021).

[21] A. A. Bogdanov, K. L. Koshelev, P. V. Kapitanova, M. V. Rybin, S. A. Gladyshev, Z. F. Sadrieva, K. B. Samusev, Y. S. Kivshar, and M. F. Limonov, *Bound States in the Continuum and Fano Resonances in the Strong Mode Coupling Regime*, Adv. Photonics **1**, 1 (2019).

[22] A. Overvig, N. Yu, and A. Alù, *Chiral Quasi-Bound States in the Continuum*, Phys. Rev. Lett. **126**, 73001 (2021).

[23] H. Nakamura, N. Hatano, S. Garmon, and T. Petrosky, *Quasibound States in the Continuum in a Two Channel Quantum Wire with an Adatom*, Phys. Rev. Lett. **99**, (2007).

[24] A. C. Overvig, S. C. Malek, M. J. Carter, S. Shrestha, and N. Yu, *Selection Rules for Quasibound States in the Continuum*, Phys. Rev. B **102**, 1 (2020).

[25] C. A. Moyer, *A Unified Theory of Quasibound States*, AIP Adv. **4**, (2014).

[26] W. Huang, S. Liu, Y. Cheng, J. Han, S. Yin, and S. Yin, *Universal Coupled Theory for Metamaterial Bound States in the Continuum*, New J. Phys. **23**, (2021).

[27] N. Solodovchenko, K. Samusev, D. Bochek, and M. Limonov, *Bound States in the Continuum in Strong-Coupling and Weak-Coupling Regimes under the Cylinder-Ring Transition*, Nanophotonics **10**, 4347 (2021).

[28] M. Kang, Z. Zhang, T. Wu, X. Zhang, Q. Xu, A. Krasnok, J. Han, and A. Alù, *Coherent Full Polarization Control Based on Bound States in the Continuum*, Nat. Commun. **13**, 1 (2022).

[29] M. S. Hwang, H. C. Lee, K. H. Kim, K. Y. Jeong, S. H. Kwon, K. Koshelev, Y. Kivshar, and H. G. Park, *Ultralow-Threshold Laser Using Super-Bound States in the Continuum*, Nat. Commun. **12**, 1 (2021).

[30] S. G. Lee, C. S. Kee, and S. H. Kim, *Bound States in the Continuum (BIC) Accompanied by Avoided Crossings in Leaky-Mode Photonic Lattices*, Nanophotonics **9**, 4373 (2020).

[31] N. J. J. Van Hoof, D. R. Abujetas, S. E. T. Ter Huurne, F. Verdelli, G. C. A. Timmermans, J. A. Sánchez-Gil, and J. G. Rivas, *Unveiling the Symmetry Protection of Bound States in the Continuum with Terahertz Near-Field Imaging*, ACS Photonics **8**, 3010 (2021).

[32] D. C. Marinica, A. G. Borisov, and S. V. Shabanov, *Bound States in the Continuum in Photonics*, Phys. Rev. Lett. **100**, (2008).

[33] F. Monticone and A. Alù, *Embedded Photonic Eigenvalues in 3D Nanostructures*, Phys. Rev. Lett. **112**, (2014).

[34] S. Longhi, *Transfer of Light Waves in Optical Waveguides via a Continuum*, Phys. Rev. A - At. Mol. Opt. Phys. **78**, 2405 (2008).

[35] D. R. Abujetas, Á. Barreda, F. Moreno, J. J. Sáenz, A. Litman, J. M. Geffrin, and J. A. Sánchez-Gil, *Brewster Quasi Bound States in the Continuum in All-Dielectric Metasurfaces from Single Magnetic-Dipole Resonance Meta-Atoms*, Sci. Rep. **9**, 1 (2019).

[36] M. Tsimokha, V. Igoshin, A. Nikitina, I. Toftul, K. Frizyuk, and M. Petrov, *Acoustic Resonators: Symmetry Classification and Multipolar Content of the Eigenmodes*, Phys. Rev. B **105**, 1 (2022).

[37] S. T. Ha, Y. H. Fu, N. K. Emani, Z. Pan, R. M. Bakker, R. Paniagua-Domínguez, and A. I. Kuznetsov, *Directional Lasing in Resonant Semiconductor Nanoantenna Arrays*, Nat. Nanotechnol. **13**, 1042 (2018).

[38] S. Joseph, S. Pandey, S. Sarkar, and J. Joseph, *Bound States in the Continuum in Resonant Nanostructures: An Overview of Engineered Materials for Tailored Applications*, Vol. 10 (2021).

[39] Y. Yu, M. Heuck, H. Hu, W. Xue, C. Peucheret, Y. Chen, L. K. Oxenløwe, K. Yvind, and J. Mørk, *Fano Resonance Control in a Photonic Crystal Structure and Its Application to Ultrafast Switching*, Appl. Phys. Lett. **105**, 1 (2014).

[40] S. I. Azzam, K. Chaudhuri, A. Lagutchev, Z. Jacob, Y. L. Kim, V. M. Shalaev, A. Boltasseva, and A. V. Kildishev, *Single and Multi-Mode Directional Lasing from Arrays of Dielectric Nanoresonators*, Laser Photonics Rev. **15**, 1 (2021).

[41] K. Hirose, Y. Liang, Y. Kurosaka, A. Watanabe, T. Sugiyama, and S. Noda, *Watt-Class High-Power, High-Beam-Quality Photonic-Crystal Lasers*, Nat. Photonics **8**, 406 (2014).

[42] J. Vučković, M. Lončar, H. Mabuchi, and A. Scherer, *Optimization of the Q Factor in Photonic Crystal Microcavities*, IEEE J. Quantum Electron. **38**, 850 (2002).

[43] X. Sun, *Photonic Integrated Circuits with Bound States in the Continuum: Principle and Applications*, Opt. InfoBase Conf. Pap. **6**, (2020).

[44] M. V. Rybin, K. L. Koshelev, Z. F. Sadrieva, K. B. Samusev, A. A. Bogdanov, M. F. Limonov, and Y. S. Kivshar, *High- Q Supercavity Modes in Subwavelength Dielectric Resonators*, Phys. Rev. Lett. **119**, 1 (2017).

[45] S. Han et al., *All-Dielectric Active Terahertz Photonics Driven by Bound States in the Continuum*, Adv. Mater. **31**, 1 (2019).

[46] B. Gallinet, A. Lovera, T. Siegfried, H. Sigg, and O. J. F. Martin, *Fano Resonant Plasmonic Systems: Functioning Principles and Applications*, AIP Conf. Proc. **1475**, 18 (2012).

[47] A. Cerjan, C. Jorg, S. Vaidya, S. Augustine, W. A. Benalcazar, C. W. Hsu, G. Von Freymann, and M. C. Rechtsman, *Observation of Bound States in the Continuum Embedded in Symmetry Bandgaps*, Sci. Adv. **7**, 3 (2021).

[48] M. S. Hwang, K. Y. Jeong, J. P. So, K. H. Kim, and H. G. Park, *Nanophotonic Nonlinear and Laser Devices Exploiting Bound States in the Continuum*, Commun. Phys. **5**, 1 (2022).

[49] D. M. Pozar, *Microwave Engineering*, Vol. 8 (1989).